Polym. Bull. (2012) 68:1565–1575
DOI 10.1007/s00289-011-0633-6

ORIGINAL PAPER

Nanofibrous ultrahigh molecular weight polyethylene synthesized using $TiCl_4$ as catalyst supported on MCM-41 and SBA-15

Dongliang Li · Jinhua Lei · Honghua Wang · Min Jiang · Guangyuan Zhou

Received: 27 February 2011 / Revised: 2 September 2011 / Accepted: 18 September 2011 /
Published online: 15 October 2011

Abstract Nanofibrous ultrahigh molecular weight polyethylene (UHMWPE) was synthesized via Ziegler–Natta catalyst anchoring on MCM-41 and SBA-15 as supported catalysts, respectively. These supported catalysts exhibited high activity at different temperatures and Al/Ti ratios, and showed different polymerization kinetics behaviors which were well explained by their different pore structures. The ultrahigh molecular weight of polyethylene might be due to the restrained spaces of the supported catalysts mesopores prohibiting the polymer chains transfer reaction. The obtained nanofibrous morphology might be for the high enough stress generated in the mesopores extruding the polymer out to form.

Keywords Ethylene polymerization · Supported catalysts · Nanofibrous UHMWPE · Polymerization kinetics

Introduction

Mesoporous molecular sieves (MMSs) were promising support materials, which had uniform pore sizes, parallel pores to the axis, high surface areas, and big pore volumes, and were natural micro-reactors for catalytic reaction [1–3]. Focused on these properties, many researchers immobilized catalysts on the mesopores of MMS for ethylene polymerization [4–9]. The most notable one among these was that Aida and coworkers [4] used MSF as support for the immobilization of Cp_2TiCl_2 and applied it for the synthesis of polyethylene nanofibers. The polymer chains growing

D. Li · J. Lei · H. Wang · M. Jiang · G. Zhou (✉)
Key Laboratory of Polymer Ecomaterials, Changchun Institute of Applied Chemistry, Chinese Academy of Sciences, 130022 Changchun, China
e-mail: gyzhou@ciac.jl.cn

D. Li
Graduate School of the Chinese Academy of Sciences, Beijing, China

in the mesopores of MSF could not fold effectively in such restrained spaces and were extruded from the mesopores to form nanofibrous morphology. $TiCl_4$ was a classical Ziegler–Natta catalyst for ethylene polymerization, which was cheap, facile, and could "drop in" the current polymerization process. In Semsarzadeh's and Aghili study [8], they used MCM-41 as support material and synthesized different catalysts with different molar ratios of Mg/Ti and detected the effect of $MgCl_2$ on catalytic activity and thermal properties of obtained polyethylene. They found that the presence of $MgCl_2$ increased the catalytic activity and gave the polyethylene with higher crystallinity and melting points. Wang [9] immobilized $TiCl_4$ indirectly on the inner pores of MCM-41 and used beta-cyclodextrin to destroy the exterior catalyst. They found the obtained PE morphology was mainly amorphous without beta-cyclodextrin. MCM-41 and SBA-15 were remarkable MMS, both of which had mesopores structure but with different diameters. In this study, we took MCM-41 and SBA-15 as support materials, respectively, to immobilize $TiCl_4$ for the synthesis of polyethylene with special property. Ordinarily, there were three methods to synthesize the $TiCl_4/MgCl_2/SiO_2$ catalyst system [10–12]. Here, we used CH_3MgCl as scavenger to remove the hydroxyl on the surface to increase the catalytic activity. We also detected the effect of pore structures on polymerization kinetics and investigated the catalysts at the temperatures and Al/Ti ratios. The obtained polyethylene showed nanofibrous morphology.

Experimental

Materials

All treatments were performed under a nitrogen atmosphere with standard Schlenk techniques. CH_3MgCl (3 mol L^{-1} in THF) was purchased from the Acros. Poly (ethylene oxide)-*block*-poly (propylene oxide)-*block*-poly (ethylene oxide) triblock copolymer (P_{123}, $EO_{20}PO_{70}EO_{20}$, $M_{avg.} = 5800$) was purchased from Aldrich, and other reagents were obtained from the local commercial markets. All solvents were treated by the MBRAUN Solvent Purification System (MB SPS-800) before using. The MCM-41 and SBA-15 were synthesized using literature methods [13, 14]. Before using, they were heated at 120 °C under vacuum for 6 h.

Preparation of supported catalyst

The $TiCl_4/MgCl_2$/MCM-41 (SC-1): 1.0 g of MCM-41 was added to the mixture of 50 mL of toluene and 10 mmol of CH_3MgCl (3 mol L^{-1} in THF). After stirring for 4 h at 50 °C, the complex support was collected and washed three times with 20 mL of toluene. Without drying, the complex support was added to a mixture of 50 mL toluene and 6 mL $TiCl_4$ at 0 °C, stirred for 0.5 h. Later, the mixture was heated to 120 °C, stirred for 2 h, then filtrated and washed three times with 20 mL toluene. Then, the obtained solid was added to a mixture of 50 mL toluene and 5 mL $TiCl_4$

again, and stirred for 2 h at 120 °C. The supported catalyst was filtrated and washed three times with 20 mL of toluene, then dried under vacuum to give a khaki powder.

The $TiCl_4/MgCl_2$/SBA-15 (SC-2) was synthesized as above mentioned. A light brown powder was obtained with SBA-15 instead of MCM-41 as support material.

Ethylene polymerization

High-pressure ethylene polymerization was carried out in a 1 L autoclave stainless-steel reactor equipped with a mechanical stirrer and a temperature controller. 500 mL of *n*-hexane and the desired amount of co-catalyst TIBA were added in order with the mechanical stirrer working at 500 rpm [1]. When heated up to the reaction temperature, the catalyst was added to the reactor, and ethylene with the desired pressure was supplied to start the polymerization. After 1 h, the polymerization was terminated by the addition of acidified ethanol. The obtained polymer was separated by filtration and dried under vacuum to constant weight.

Characterization of support, catalyst, and polymers

The supported catalysts (SC-1 and SC-2) and support materials (MCM-41 and SBA-15) were characterized by X-ray diffraction (XRD) and N_2 absorption/desorption isotherms. XRD measurement was performed on a Bruck D8 X-ray Thin Firm Reflector at 293 K using Cu-Kα radiation at 40 kV and 35 mA. The N_2 absorption/desorption isotherms were measured with NOVA-1000 at 77 K. The surface areas, pore volume, and average pore diameter were calculated with the NOVA Enhanced Data Reduction Software Ver.2.13.

The loading of titanium and magnesium in the supported catalyst was determined by ICP-AES measurements. A mass flowmeter was installed at the ethylene intake of autoclave to record in situ ethylene flow. The molecular weight of the obtained polyethylene was determined by intrinsic viscosity measurements in decahydronaphthalene at 135 °C with an Ubbelohde viscometer by a one-point method [15]. The polymers were characterized with a Perkin-Elmer 7 Series thermal analysis system with a heating ratio of 10 °C min^{-1} in the range from 40 to 160 °C. The melting points measured in the first and second heating process were obtained. The SEM measurement of the obtained polyethylene morphology was carried out with a Philips XL30 device.

Results and discussion

Characterization of supports and the supported catalysts

As shown in Fig. 1, the XRD pattern for MCM-41 and SBA-15 showed three characteristic diffraction peaks that were indexed as (100), (110), (200), indicating the support materials had parallel hexagonal channel structures. After supporting $TiCl_4$, the characteristic diffraction peaks for supported catalysts (SC-1, SC-2) on (110) and (200) became weaker, but the characteristic diffraction peak on (100)

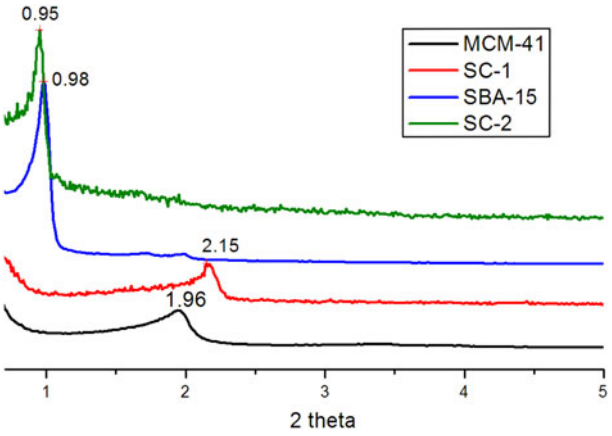

Fig. 1 The XRD patterns of support materials and supported catalysts

Table 1 The structural parameters[a] of support materials and supported catalysts

Sample	S_{BET}/(m^2 g^{-1})	V_p/(mL g^{-1})	d_p/nm
MCM-41	933.0	0.884	3.788
SC-1	414.5	0.416	3.736
SBA-15	559.3	0.654	4.677
SC-2	290.6	0.319	4.199

[a] S_{BET} BET specific surface area; *Vp* specific pore volume; *dp* average pore diameter, obtained from BJH adsorption data

remained strong. The reduced intensity for supported catalysts (SC-1, SC-2) could be explained by the catalyst existing on the mesopores of MCM-41 and SBA-15.

The N_2 absorption/desorption measurements for support materials and supported catalysts were taken under the same condition. The results of surface area, pore volume, and average pore size for support materials and supported catalysts were listed in Table 1. From Table 1, we found that the surface area, pore volume, and average pore size of supported catalysts SC-1 and SC-2 decreased comparing with MCM-41 and SBA-15, respectively, indicating that the catalyst had been immobilized on the mesopores of MCM-41 and SBA-15. The pore size distributions for support materials and supported catalysts were showed in the Fig. 2. As shown in Fig. 2, after immobilizing, the SC-1 and SC-2 still had narrow pore size distributions.

The loading amounts of titanium and magnesium in SC-1 and SC-2 were determined by ICP-AES measurements, and the results were listed in Table 2. The Mg/Ti for both SC-1 and SC-2 was nearly 2.0, which was reported to be a reasonable ratio for high polymerization activity [11, 12].

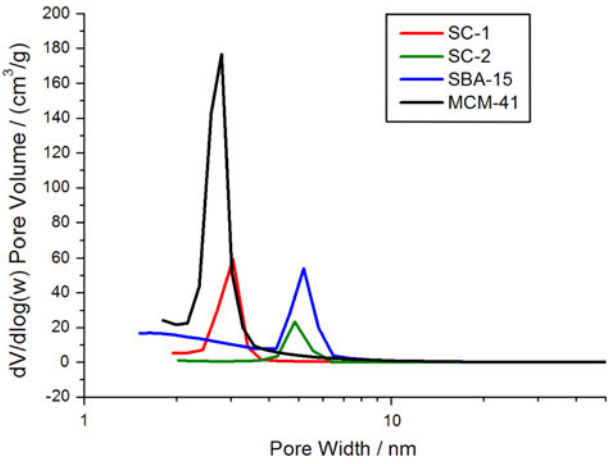

Fig. 2 The pore size distribution of support materials and supported catalysts

Table 2 Ti and Mg contents of SC-1 and SC-2

Sample	Mass fraction/%		Mg/Ti mole ratio
	Ti	Mg	
SC-1	7.80	7.73	1.95
SC-2	5.53	6.61	0.35

Ethylene polymerization and polyethylene characterization

Ethylene polymerization was carried out with SC-1 or SC-2 as catalyst, respectively, with TIBA as cocatalyst. The polymerization results were listed in Table 3. $TiCl_4/MgCl_2$ catalyst system was also introduced for comparison, and the result was listed as Run 19 in Table 3.

$TiCl_4/MgCl_2$ catalyst system was a highly activated catalyst for the synthesis of ultrahigh molecular weight polyethylene (UHMWPE). Under our polymerization condition, the obtained polyethylene using $TiCl_4/MgCl_2$ catalyst had an ultra-high molecular weight of 2.89×10^6 g mol^{-1}. After immobilizing on the mesopores of MCM-41 or SBA-15, the supported catalysts exhibited a different polymerization behavior and gave different results. From Table 3, we found the obtained polyethylene synthesized using SC-1 catalyst, from Run 1 to Run 9, had ultrahigh molecular weight from 3.5×10^6 to 5.7×10^6 g mol^{-1} and the obtained polyethylene synthesized using SC-2 catalyst, from Run 10 to Run 18, had ultra-high molecular weight from 3.9×10^6 to 5.7×10^6 g mol^{-1}. The higher molecular weight could be explained by the restrained spaces in the mesopores of support materials prohibiting the polymer chains transfer reaction. In Kim's study [16], the excess growth polymers in the AAO micropores generated a high enough stress to extrude polymer out to form a similar nanofibrous morphology. At the same time, the excess growth polymer confined the ethylene diffusing to the inner AAO

Table 3 The results of ethylene polymerization[a] with SC-1 and SC-2 as catalyst

Run	Catalyst	T_r/°C	Al/Ti ratio	Act./kg PE (gcat)$^{-1}$	Melting points				Mv/10^4 g mol^{-1}
					$T_{m.first}$/°C	Crys./%	$T_{m\cdot sec}$/°C	Crys./%	
1	SC-1	50	360	1.7	143.5	65.4	135.4	45.3	575
2		60	360	2.0	143.6	62.1	135.4	42.8	409
3		77	360	2.9	142.4	64.6	135.4	48.5	400
4		90	360	2.9	142.4	62.2	135.6	46.4	341
5		77	120	1.7	142.7	65.4	135.6	47.2	399
6		77	240	2.5	142.4	66.0	135.5	50.5	415
7		77	480	3.3	142.3	63.7	135.5	48.3	384
8		77	600	3.5	142.6	63.6	135.8	43.9	351
9		77	720	2.9	142.3	70.1	136.1	54.3	332
10	SC-2	50	400	3.3	144.1	65.8	135.3	44.5	571
11		65	400	4.2	143.9	61.0	135.6	43.8	510
12		77	400	5.3	143.9	61.4	136.3	47.7	411
13		90	400	6.4	143.0	65.5	135.9	45.8	315
14		77	240	1.5	144.2	64.4	136.5	48.5	453
15		77	320	2.4	144.2	68.8	135.5	47.9	445
16		77	360	5.8	142.9	63.7	135.5	43.8	430
17		77	480	4.7	143.0	65.1	135.5	48.4	412
18		77	560	2.9	143.8	63.3	136.0	45.8	389
19	$TiCl_4$/$MgCl_2$	77	360	6.8	143.4	60.7	136.9	45.7	289

[a]Polymerization conditions: solvent = 500 mL hexane, catalyst = 10 mg SC-1 or SC-2, pressure = 10 atm ethylene, time = 1 h

micropores and gave a microfiber with 10–20 μm length. MCM-41 and SBA-15 had parallel hexagonal mesopores with diameter from 3.87 to 4.7 nm which were much smaller than the AAO diameter. During polymerization, the ethylene diffused to active sites continuously to induce polymer chains growth. After the mesopores were filled with excess polymer, the ethylene diffusion became slow and difficult. The restrained spaces in the mesopores prohibited the polymer chain transfer reaction.

The UHMWPE synthesized by SC-1 and SC-2 also had high crystallinity. The UHMWPE synthesized using SC-1 catalyst, from Run 1 to Run 9, had crystallinity from 62.1 to 70.1% and the UHMWPE synthesized using SC-2 catalyst, from Run 9 to Run 16, had crystallinity from 61.0 to 68.8%.

The activities of supported catalysts SC-1 and SC-2 for ethylene polymerization were about 40–95% of the $TiCl_4/MgCl_2$ catalyst. These could be attributed to the mesopores of support materials prohibiting the monomer to diffuse to the activated sites. Both SC-1 and SC-2 showed decay kinetics behaviors during polymerization. Taken Run 3 and Run 16, for example, as shown in Fig. 3, in the initial stage, the supported catalyst SC-1 consumed ethylene drastically, reaching to the top activity

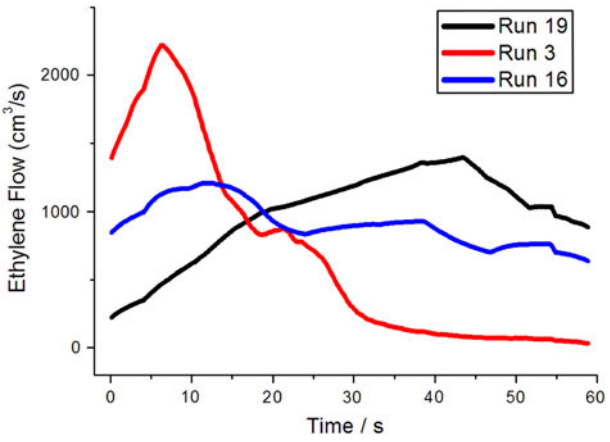

Fig. 3 The polymerization kinetic curves of Run 3, Run 16, and Run 19

in 10 min. After 15 min, the ethylene flow decreased to half of the top sharply. After 30 min, the ethylene flow decreased to near zero, indicating the SC-1 was deactivated. The supported catalyst SC-2 showed a smoothly decay kinetics curve. In the initial stage, the ethylene flow increased smoothly compared with SC-1. After 30 min, the SC-2 still had 70% of the top activity and kept to the end. For comparison, $TiCl_4/MgCl_2$ catalyst system exhibited a relative developed polymerization kinetic as Run 19 showed in Fig. 3. These differences could be explained by the property of support materials. MCM-41 and SBA-15 as support materials had larger surface area and stronger configuration intensity than amorphous $MgCl_2$. The supported catalyst SC-1 had the largest surface area and exposed the most activated sites in the initial stage of polymerization. Ethylene diffused to the activated sites and grew to give drastic ethylene consumption. When mesopores were filled with polymer, ethylene diffusion to the activated sites became difficult, and ethylene flow decreased sharply. The supported catalyst SC-2 had moderate surface area and the ethylene consumption increased slowly than SC-1 in the initial stage of polymerization. For that SC-2 had bigger pore diameter than SC-1, after 20 min, the ethylene could still diffuse to the active sites to grow. Amorphous $MgCl_2$ had weaker configuration intensity than MCM-41 and SBA-15. During polymerization, the $TiCl_4/MgCl_2$ catalyst broke up gradually, and the released activated sites increased in order of magnitude, so the ethylene consumption increased to give a developing kinetics curve.

The SC-1 and SC-2 catalysts were also investigated at different temperatures and Al/Ti ratios, and gave similar results. The activity increased along with the polymerization temperature rising. At 90 °C, SC-2 exhibited high activity up to 6.4 kg PE $(gcat)^{-1}$, almost double more than the activity at 50 °C, while the molecular weight decreased from 5.7 to 3.4 $\times$ 10^6 g mol^{-1} as shown in Fig. 4a. As we know, high temperature accelerated the polymer chains grow reaction that benefited for high activity. While, high temperature also increased the polymer chains transferring to β-H that would induce to short average life of active sites and

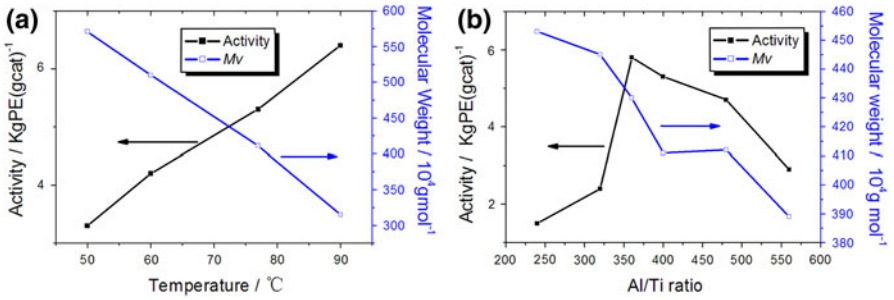

Fig. 4 The influences of temperature (**a**) and Al/Ti ratios (**b**) on activity and molecular weight for SC-2

lower polymer molecular weight. Under the same temperature and different Al/Ti ratios, the catalysts exhibited different activities and produced UHMWPE with different molecular weight. In Fig. 4b, SC-2 showed the highest activity with Al/Ti value 400. With more or less TIBA, SC-2 showed a lower activity. The molecular weight of UHMWPE decreased with higher Al/Ti ratio and got the least Mv with Al/Ti ratio value 560. Compared with Al/Ti ratios, polymerization temperature made a more influence on the activity and polymer molecular weight. Figure 5 showed the effect of polymerization temperature and Al/Ti ratios on the SC-1 activity and polymer molecular weight. With the same Al/Ti ratio value 360, SC-1 showed highest activity at 77 and 90 °C that might be for that the accelerated polymer chains grow reaction was counteracted by the increased polymer chains transfer reaction. While the polymer molecular weight still decreased at higher temperature. At the same temperature, SC-1 showed highest polymer molecular weight with Al/Ti ratio value 240 that might be for most of the polymer growing at the active sites on the outsides of the mesopores with lower Al/Ti ratio.

The morphology measurements of UHMWPE were carried out using a Philips XL30 device with an accelerating voltage 20 kV. Figure 6a–c showed the SEM images of the nanofibrous UHMWPE synthesized using SC-1 with different Al/Ti ratios. Under different Al/Ti ratios, the SC-1 showed different catalytic activities, but the obtained UHMWPE showed similar nanofibrous morphology. With high activity, the excess growth polymer inside generated a high enough stress to extrude

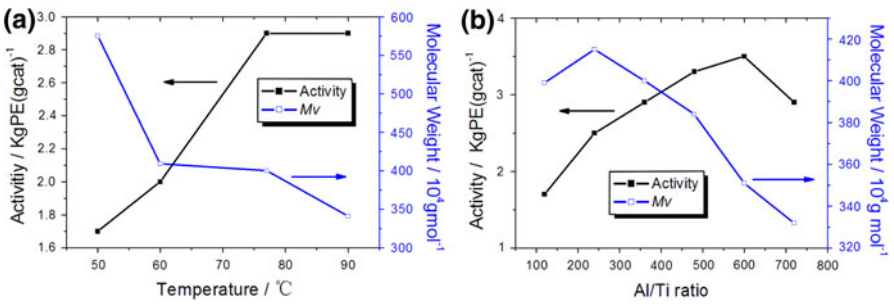

Fig. 5 The influences of temperature (**a**) and Al/Ti ratios (**b**) on activity and molecular weight for SC-1

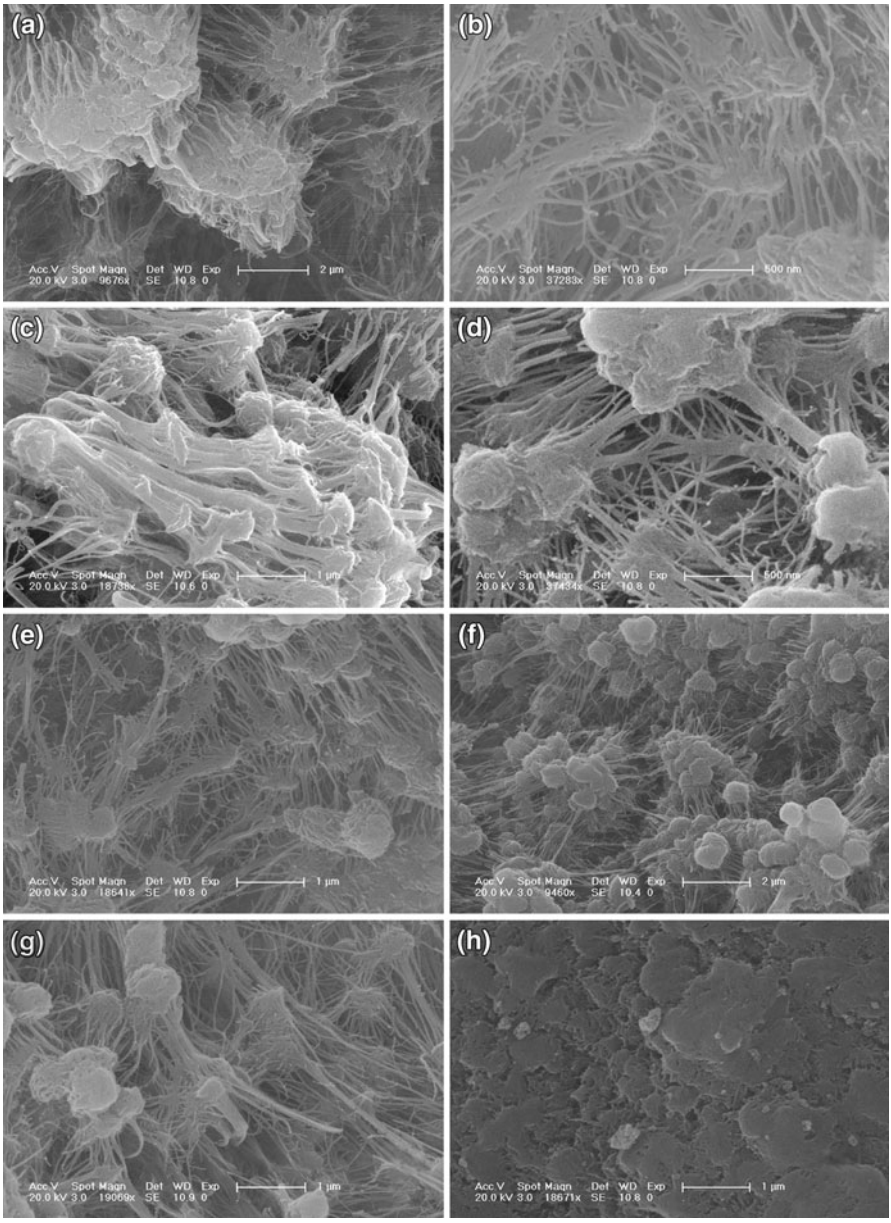

Fig. 6 The SEM images of nanofibrous UHMWPE synthesized using SC-1 and SC-2 catalysts with different Al/Ti ratios and polymerization temperatures. **a** Run 5; **b** Run 3; **c** Run 8; **d** Run 10; **e** Run 11; **f** Run 12; **g** Run 13; and **h** Run 19

them out to form similar nanofibrous morphology. Figure 6d–g showed the nanofibrous UHMWPE synthesized using SC-2 at different temperatures. At different temperatures, even high temperature, the nanofibrous morphology could be formed, which would be benefited from the strong configuration of SBA-15 at

different temperatures. These UHMWPE nanofibers synthesized using SC-1 and SC-2 had similar diameter, even the SC-1 and SC-2 had different diameters. It might be for the polymer chains extruding from the mesopores of SC-1 or SC-2 and assembling to similar size nanofibers. At the same time, they also contained some similar morphology, clew-like particles in size of 1–2 μm. These particles were formed by nanofibers interweaving with each other. From these images, it could be observed that, some particles had smooth surface, which might be for that the polymer growing at active sites on the outer surface covered the supported catalysts in the initial stage and the polymer growing from the inner pores were too weak to breach this film. Some other particles had distinct clew-like morphology and lots of nanofibers existed between these particles. For comparison, the SEM images of UHMWPE synthesized using $TiCl_4/MgCl_2$ catalyst under our condition were also shown in Fig. 6h. Some short nanofibers were observed since some nanopores or micropores existed in the amorphous $MgCl_2$. However, with the amorphous $MgCl_2$ breaking up gradually during polymerization, the major morphology of obtained UHMWPE was nanosheets.

Conclusion

The nanofibrous UHMWPE were synthesized using supported catalysts SC-1 and SC-2. The pore structures of supported catalysts were determined by XRD and BET and the results indicated $TiCl_4$ had been immobilized on the mesopores. The supported catalysts SC-1 and SC-2 exhibited decay kinetics behaviors during polymerization. The supported catalyst SC-1 consumed the more rapid ethylene flow in the initial stage for its larger surface area and SC-2 showed a smoothly decay kinetics behavior for its moderate surface area and bigger pore diameter. SC-1 and SC-2 were also investigated under different temperatures and Al/Ti ratios and showed similar results. The catalytic activity reached the highest at high temperature and the molecular weight reached the highest at low temperature and low Al/Ti ratio. Compared with the UHMWPE synthesized by $TiCl_4/MgCl_2$, the higher molecular weight of nanofibrous UHMWPE could be explained by the restrained spaces of the support materials mesopores prohibiting the polymer chains transfer reaction. The nanofibrous morphology of obtained UHMWPE might be for the high enough stress generated in the mesopores extruding the polymer out to form.

References

1. Corma A, Garcia H, Moussaif A, Sabater MJ, Zniber R, Redouane A (2002) Chiral copper(II) bisoxazoline covalently anchored to silica and mesoporous MCM-41 as a heterogeneous catalyst for the enantioselective Friedel-Crafts hydroxyalkylation. Chem Commun 10:1058
2. Crudden CM, Sateesh M, Lewis R (2005) Mercaptopropyl-modified mesoporous silica: a remarkable support for the preparation of a reusable, heterogeneous palladium catalyst for coupling reactions. J Am Chem Soc 127:10045

3. Karimi B, Abedi S, Clark JH, Budarin V (2006) Highly efficient aerobic oxidation of alcohols using a recoverable catalyst: the role of mesoporous channels of SBA-15 in stabilizing palladium nanoparticles. Angew Chem Int Ed 45:4776
4. Kageyama K, Tamazawa J, Aida T (1999) Extrusion polymerization: catalyzed synthesis of crystalline linear polyethylene nanofibers within a mesoporous silica. Science 285:2113
5. Ye ZB, Zhu SP, Wang WJ, Alsyouri H, Lin YS (2003) Morphological and mechanical properties of nascent polyethylene fibers produced via ethylene extrusion polymerization with a metallocene catalyst supported on MCM-41 particles. J Polym Sci B Polym Phys 41:2433
6. Dong XC, Wang L, Jiang GH, Zhao ZR, Sun TX, Yu HJ, Wang WQ (2005) MCM-41 and SBA-15 supported Cp_2ZrCl_2 catalysts for the preparation of nano-polyethylene fibres via in situ ethylene extrusion polymerization. J Mol Catal A Chem 240:239
7. Guo C, Zhang D, Wang FS, Jin GX (2005) Nanofibers of polyethylene produced by SBA-15 supported zirconium catalyst [*N*-(3-tert-butylsalicylidene)-4′-allyloxylanilinato]$_2$Zr(IV)Cl_2. J Catal 234:356
8. Semsarzadeh MA, Aghili A (2008) Novel preparation of polyethylene from nano-extrusion polymerization inside the nanochannels of MCM-41/$MgCl_2$/$TiCl_4$ catalysts. J Macromol Sci A Pure Appl Chem 45:680
9. Dong XC, Wang L, Zhou JF, Yu HJ, Sun TX (2006) Preparation of nano-polyethylene fibres using $TiCl_4$/MCM-41 catalytic system. Catal Commun 7:1
10. Soga K, Ohnishi R, Sano T (1982) Copolymerization of ethylene and propylene over the SiO_2 supported $MgCl_2$/$TiCl_3$ catalyst. Polym Bull 7:547
11. Kim I, Kim JH, Woo SI (1990) Kinetic study of ethylene polymerization by highly active silica supported $TiCl_4$/$MgCl_2$ catalysts. J Appl Polym Sci 39:837
12. Lu HL, Xiao SJ (1993) Structure and behavior of SiO_2/$MgCl_2$ bisupported Ziegler-Natta catalysts for olefin polymerization. Makromol Chem Macromol Chem Phys 194:421
13. Beck JS, Vartuli JC, Roth WJ, Leonowicz ME, Kresge CT, Schmitt KD, Chu CTW, Olson DH, Sheppard EW, McCullen SB, Higgins JB, Schlenker JL (1992) A new family of mesoporous molecular sieves prepared with liquid crystal templates. J Am Chem Soc 114:10834
14. Zhao DY, Feng JL, Huo QS, Melosh N, Fredrickson GH, Chmelka BF, Stucky GD (1998) Triblock copolymer syntheses of mesoporous silica with periodic 50 to 300 angstrom pores. Science 279:548
15. Wirick MG, Elliott JH (1973) One-point intrinsic viscosity method for hydroxyethylcellulose, hydroxypropylcellulose and sodium carboxymethylcellulose. J Appl Polym Sci 17:2867
16. Nair S, Naredi P, Kim SH (2005) Formation of high-stress phase and extrusion of polyethylene due to nanoconfinements during Ziegler-Natta polymerization inside nanochannels. J Phys Chem B 109:12491